

# Information transmission and recovery in neural communication channels revisited

P. H. E. Tiesinga

*Sloan-Swartz Center for Theoretical Neurobiology and Computational Neurobiology Laboratory, Salk Institute,  
10010 North Torrey Pines Road, La Jolla, California 92037.*

(Received 19 February 2001; published 20 June 2001)

Nerve cells in the brain generate all-or-none electric events—spikes—that are transmitted to other nerve cells via chemical synapses. An important issue in neuroscience is how neurons encode and transmit information using spike trains. Recently, signal transduction through two neurons connected by an excitatory chemical synapse was studied by Eguia *et al.* [Phys. Rev. E **62**, 7111 (2000)]. They reported an apparent violation of the data processing inequality: The mutual information between the input signal and the output of the first neuron can be lower than the mutual information between the input signal and the output of the second neuron, that only receives input from the first neuron. We investigate whether it is possible, using a different method, to retrieve, from the first neuron's spike train, all the information about the input that is present in the second neuron's output. We find that single interspike intervals (ISI's) from the first neuron, at a resolution of 0.5 time units, contain more information about the input signal than those of the second neuron. Using a classification procedure based on the ISI return map, we recover 71% of the input entropy using the first neuron's spike train, and only 42% using the second neuron's spike train. Hence for these spike-train observables the data processing inequality is not violated.

DOI: 10.1103/PhysRevE.64.012901

PACS number(s): 87.10.+e, 89.70.+c, 05.45.-a

## I. INTRODUCTION

The brain consists of a large number of interconnected neurons. Neurons generate trains of action potentials, spikes, that are transmitted to other neurons via chemical synapses. There is an ongoing debate whether the precise spike times encode information, or whether only the average spike rate is informative (see, for instance, Ref. [1]). It is therefore important to theoretically study how information can be encoded in spike trains, and what part can be transmitted across synapses. Eguia, Rabinovich, and Abarbanel [2] (abbreviated ERA in the remainder of the report) studied the transmission of a pulsatile current injected in the first neuron, that projects to the second neuron via an excitatory chemical synapse, into the output spike train of the second neuron. They found that while information is hidden in the output spike train of the first neuron, it is actually transmitted to the second neuron, and can be reconstructed on the basis of its output spike train. They showed that this leads to an apparent violation of the data processing inequality [3]: The mutual information between the input and the first neuron is lower than that between the input and the second neuron.

The data processing inequality is an exact mathematical identity for variables that form a Markov chain [7]. Consider the variables  $X$  (the signal),  $Y$  (the output of neuron 1), and  $Z$  (the output of neuron 2).  $X \rightarrow Y \rightarrow Z$  form a Markov chain, when  $Y$  is a function of  $X$ ,  $Y = f(X) + h_1$  and  $Z$  is a function of  $Y$ ,  $Z = g(Y) + h_2$  [here  $h_1$  and  $h_2$  are arbitrary functions that do not depend on  $X$  or  $Y$ : the mutual information  $I(X, h_1)$ ,  $I(X, h_2)$ , and  $I(Y, h_2)$  is zero]. The mutual information between  $Z$  and  $X$  is then smaller than or equal to the mutual information between  $Y$  and  $X$ ,  $I(X, Z) = I(X, g(Y) + h_2) \leq I(X, Y)$  [7]. In numerical work the inequality may be violated. For instance, in calculating the output spike train a subthreshold signal might be thresholded away, though it might still be transmitted across the synapse. Then the assumption that  $X \rightarrow Y \rightarrow Z$  form a Markov chain is violated.

Furthermore, to calculate the entropy numerically the variables  $X$ ,  $Y$ , and  $Z$  need to be discretized into bins of width  $dX$ ,  $dY$ , and  $dZ$ , respectively. When the signal dependent part of  $Y$  is smaller than  $dY$ , but the signal dependent part in  $Z$  is larger than  $dZ$ , the data processing inequality would be violated. Here we analyze the results presented by ERA using the time series of interspike intervals (ISI's) of neurons 1 and 2. We find that the mutual information between the ISI of neuron 1 and the input signal is higher than that of the ISI of neuron 2 and the input. Furthermore, we find that the information is present at a finer temporal resolution and a larger word length (the number of bins in a symbol) than studied by ERA.

We first reproduce the results presented in Fig. 2 of ERA, and discuss the biophysical basis for the recovery of hidden information. Then we discuss how the input can be reconstructed based on interspike intervals. We conclude with a discussion of the biophysical properties of the synapse model used by ERA.

## II. RESULTS

### A. Biophysical basis for information recovery

In Fig. 1 we have reproduced the results shown in Fig. 2 of ERA for a different input spike train. The dynamical equations were like those of ERA, and a subset of them was listed in Refs. [5,6]. A synaptic current  $J_1$  consisting of nine pulses was injected into the neuron 1 [Fig. 1(A), curve  $a$ ]. In "burst coding space" events are defined as hyperpolarizations in the membrane potential  $x$ , that cross the threshold  $x_{thr} = -1$  from above. Only two pulses were transduced into a hyperpolarization of the first neuron that went below  $x_{thr} = -1$  [Fig. 1(A), curve  $b$ ], whereas in the second neuron eight of the nine pulses could be identified as events in the membrane potential  $x$  [Fig. 1(A), curve  $c$ ]. Hence the data processing inequality is violated in burst coding space as reported by ERA. Although the third pulse [Fig. 1(B), curve  $a$ ] was not

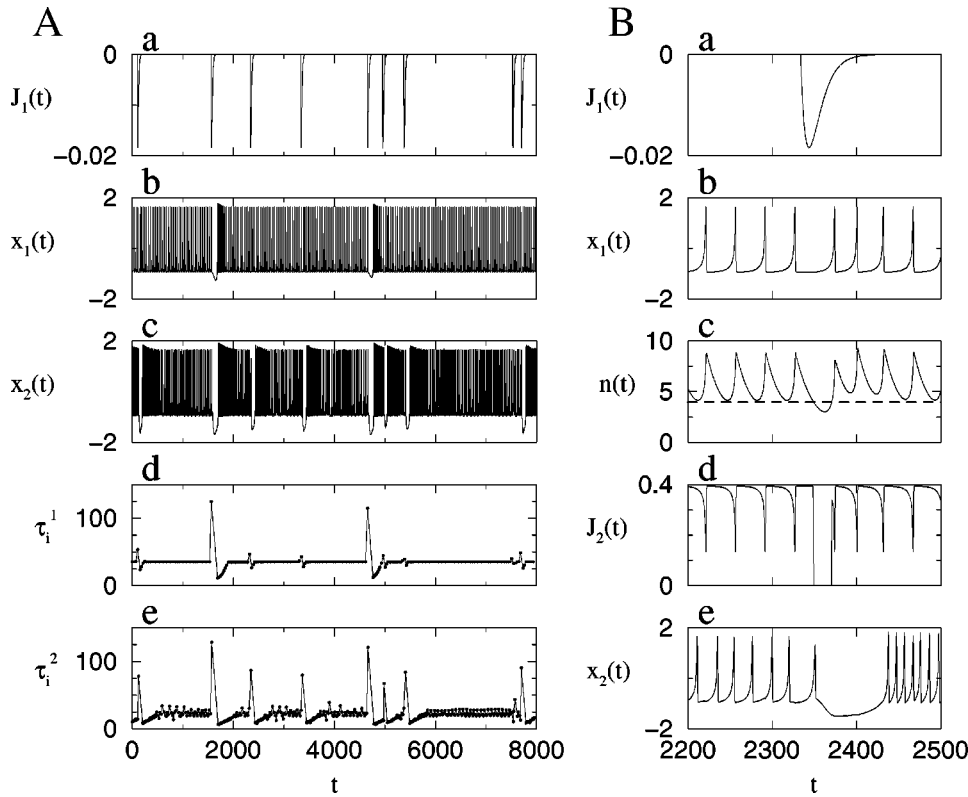


FIG. 1. (A) The synaptic input current  $J_1$  (curve *a*), the membrane potential  $x_1$  of the first neuron (curve *b*), and  $x_2$  of the second neuron (curve *c*), and the interspike intervals of neuron 1,  $\tau_i^1$ , (curve *d*) and neuron 2,  $\tau_i^2$  (curve *e*), are plotted as functions of time  $t$ . (B) Curve *a* ( $J_1$ ), *b* ( $x_1$ ), *c* [the neurotransmitter concentration  $n(t)$ ], *d* the synaptic current  $J_2$  to neuron 2, and *e*  $x_2$  vs time. In curve *c* the threshold concentration  $n_0 = 4$  (dashed line) is also plotted. Parameter values are given in Ref. [5].

transduced into a visible hyperpolarization in neuron 1, it did increase the interspike interval [Fig. 1(B), curve *b*], and the membrane potential was close to (but above)  $x_{thr} = -1$  for a longer time. As a result, the neurotransmitter concentration dropped below the threshold,  $n_0 = 4$ , of the synaptic conductance [Fig. 1(B), curve *c*] and the synaptic current dropped from  $J_2 \approx 0.4$  to zero [Fig. 1(B), curve *d*]. This “inhibitory” pulse in  $J_2$  is a factor 20 larger than the one in  $J_1$ , and hence caused a large increase in the interspike interval of neuron 2 and a pronounced hyperpolarization [Fig. 1(B), curve *e*].

The signal transduction mechanism is therefore as follows. Increases in the ISI of the first neuron are a reliable indicator of the presence and time of an inhibitory pulse. The threshold  $n_0$  was tuned so that a small increase in the ISI caused  $n$  to drop below  $n_0$ , leading to a large reduction in the synaptic current into neuron 2, but for the unperturbed ISI  $n$  always stayed above  $n_0$ .

The amount of hyperpolarization induced by the signal depends on the value of the internal neuronal variables  $y$ ,  $z$ , and  $w$ , that vary in time. Hence, depending on the arrival time of the input pulse, a small or large hyperpolarization was induced. The probability for a large hyperpolarization increased with increasing pulse amplitude. For  $J_0 = -0.05$  in the first neuron, the probability was quite low. Since the amplitude of  $J_2$  is about a factor 20 larger than  $J_1$ , the signal-induced reduction in  $n(t)$  reliably induced a hyperpolarization below  $x_{thr} = -1$  in neuron 2. Thus the biophysical substrate for the recovery of hidden information is the higher gain of the second synapse compared to the first one.

### B. Mutual information analysis

Each presynaptic pulse in  $J_1$  led to an increase in the current interspike interval of neuron 1,  $\tau_i^1 = t_{i+1}^1 - t_i^1$  [Fig.

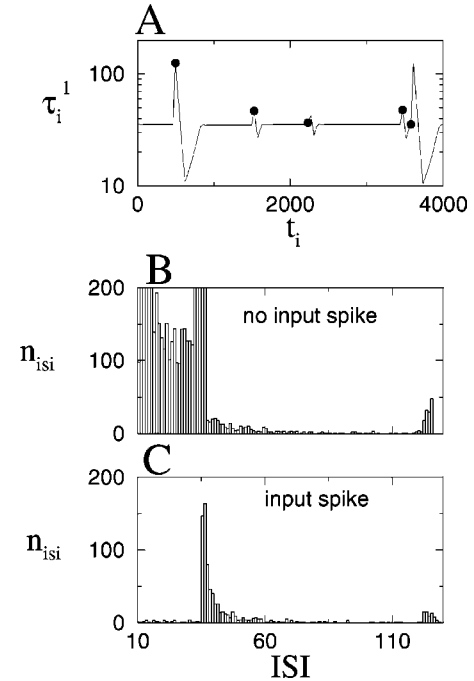


FIG. 2. Interspike intervals of neuron 1 contain information about the input. The interspike interval  $\tau_i^1$  is plotted vs its starting time  $t_i$  (solid line); the presence of an input pulse during the interval is indicated with a filled circle. Also shown is the histogram of ISI values during which (B) no input pulse occurred, and (C) an input pulse occurred; the bin width is 0.5. For clarity, bin entries  $n_{ISI}$  above 200 were cut off in the graph. During a simulation run of  $8 \times 10^5$  time units, 805 input pulses were injected, resulting in 23595 interspike intervals for neuron 1 and 38897 for neuron 2. Model parameters are given in the text and in Ref. [5].

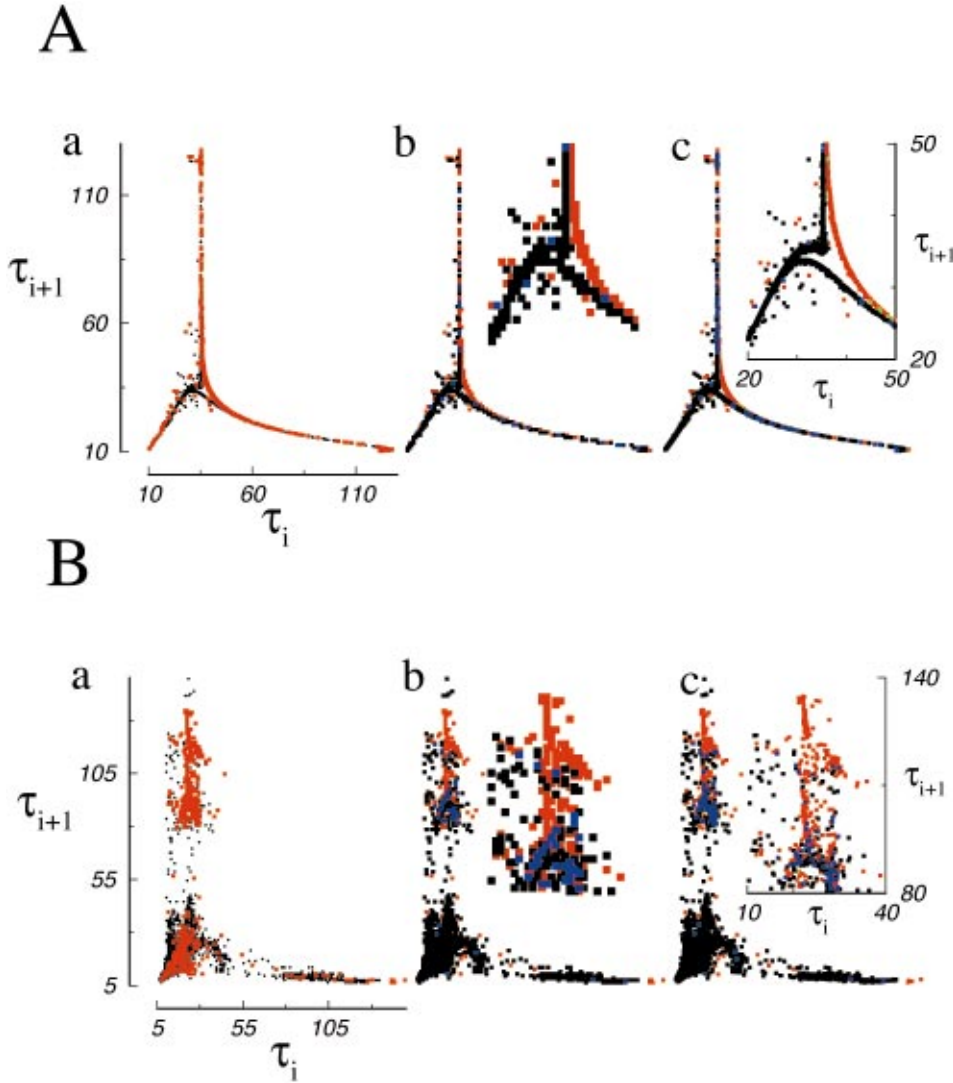


FIG. 3. (Color) Classification procedure using the return map for (A) neuron 1 and (B) neuron 2. The data are the same as in Fig. 2.  $(\tau_i, \tau_{i+1})$  was assigned a variable  $n_i$  and classification  $c_i$ , where  $n_i = 1$ , when there was an input pulse during interval  $\tau_i$ , and  $n_i = 0$  otherwise.  $(\tau_i, \tau_{i+1})$  was divided into a two-dimensional set of bins  $(k, l)$  with a height and width equal to 1. The number of points in bin  $(k, l)$  with  $n = 0$ ,  $\alpha_{kl}$ , and  $n = 1$ ,  $\beta_{kl}$ , was determined. When  $(\tau_i, \tau_{i+1})$  fell in bin  $(k, l)$ , it was classified as  $c_i = 1$  when  $\beta_{kl} \geq \alpha_{kl}$ , and  $c_i = 0$  otherwise. Curve *a*: The return map,  $n_i = 0$  (black symbols) and  $n_i = 1$  (red symbols). Curve *b*: The classification bins  $(k, l)$  color coded according to  $\beta_{kl} > \alpha_{kl}$  (red),  $\beta_{kl} < \alpha_{kl}$  (black) and  $\beta_{kl} = \alpha_{kl}$  (blue). Curve *c*: Results of the classification procedure; each  $(\tau_i, \tau_{i+1})$  is color coded,  $n_i = 1, c_i = 1$  (red),  $n_i = 0, c_i = 0$  (black),  $n_i = 1, c_i = 0$  (green), and  $n_i = 0, c_i = 1$  (blue). The insets in curves *b* and *c* are close-ups.

2(A)]. Here  $t_i^1$  is the  $i$ th spike time of neuron 1. For simplicity, the superscripts 1, 2 on  $\tau$  are suppressed in the following. A variable  $n_i$  was assigned to each  $\tau_i$ ,  $n_i = 1$  when there was an input pulse during the interval  $\tau_i$  (i.e., between  $t_i^1$  and  $t_{i+1}^1$ ), and  $n_i = 0$ , otherwise. The mutual information between  $\tau_i$  and  $n_i$  was  $M_{ISI} = S_{ISI} - [(1 - p_1)S_{ISI,0} + p_1 S_{ISI,1}]$ ,  $p_1$  was the fraction of interspike intervals with  $n_i = 1$ ,  $S_{ISI} = -\sum_{\tau} p_{ISI}(\tau) \log_2 p_{ISI}(\tau)$ , and  $S_{ISI,n} = -\sum_{\tau} p_{ISI,n}(\tau) \log_2 p_{ISI,n}(\tau)$ ;  $p_{ISI}$  was the binned histogram of all interspike intervals, and its sum was normalized to 1. Likewise,  $p_{ISI,n}$  was the normalized histogram of interspike intervals with  $n_i = n$  and  $n = 0$  or 1 [Figs. 2(B) and 2(C)]. The entropy of the input signal is  $S_{input} = -(1 - p_1) \log_2 (1 - p_1) - p_1 \log_2 p_1$ . For the example considered here,  $S_{input} = 0.215$  bits per interval, and  $M_{ISI}/S_{input} = 0.446$ .

An input pulse to neuron 1 did not always result in an increase of the ISI of the second neuron during which the pulse occurred. Instead, the next interval or the one after that was increased. Therefore, we took the mean of three consecutive ISI's as the spike-train observable  $\tau^*$ . The mutual information  $M'_{ISI}$  between  $\tau^*$  and  $n$  was calculated as before, yielding  $M'_{ISI}/S'_{input} = 0.362$ .

More information could be recovered from the first neuron's spike train by considering two consecutive ISI's (Fig. 3). Each point  $(\tau_i, \tau_{i+1})$  was characterized by  $n_i$ , and its classification  $c_i$ .  $c_i = 1$  when it was classified as having an input pulse during interval  $\tau_i$  and  $c_i = 0$  otherwise [Figs. 3(A), curve *c*, and 3(B), curve *c*].  $q_c$  is the number of intervals with  $c_i = c$ ,  $q_{nc}$  is the number of intervals with both  $n_i = n$ , and  $c_i = c$ . The mutual information between the input variable  $n$  and classification variable  $c$  was given by

$$M_{class} = S_{input} + (1 - \hat{p}_1) [p_{00} \log_2 p_{00} + (1 - p_{00}) \log_2 \times (1 - p_{00})] + \hat{p}_1 [p_{11} \log_2 p_{11} + (1 - p_{11}) \log_2 \times (1 - p_{11})]. \quad (1)$$

Here  $p_{00} = q_{00}/q_0$ ,  $p_{11} = q_{11}/q_1$ ,  $\hat{p}_1$  is the fraction of intervals classified as event, and  $S_{input}$  was as defined above. For the example in Fig. 3, we obtained  $M_{class}/S_{input} = 0.708$  for the first neuron with a bin size of  $1 \times 1$ , and  $M'_{class}/S'_{input} = 0.423$  for the second neuron.

For the example considered here the data processing inequality is not violated, whereas in the work of ERA it is

violated for the same model parameters. In the work of ERA, a temporal resolution between 3 and 30 was used, with a word size up to 16 for the spike-based mutual information. The coding fraction, the mutual information divided by the input entropy, varied between  $10^{-3}$  and 0.4. Here the coding fraction, based on a single ISI, was close to their upper range. Our calculation took into account spike timing at a resolution of  $\Delta t=0.5$ ; for equivalent accuracy the word length in the work of ERA should be  $ISI/\Delta t > 70$ . Hence we infer that the calculations of ERA were not performed at a high enough temporal resolution to extract all the information in neuron 1's spike train. Our results show that for zero noise most of the information about the input can be extracted from the spike train of neuron 1 [6].

### C. Biophysics of synaptic signal transduction

A presynaptic action potential, arriving at a presynaptic terminal, leads to neurotransmitter release across the synaptic cleft, opening ionic channels in the postsynaptic membrane. The resulting synaptic current in the postsynaptic neuron is a product of the conductance  $g_{syn}$  of the opened channels and the electric driving force  $x_{rev} - x_{post}$ . Here  $x_{rev}$  is the reversal potential, and  $x_{post}$  is the membrane potential of the postsynaptic neuron. The published synapse model of ERA [5] has three features that do not completely account for current physiological data (see Ref. [4] for models of synaptic transmission). First, the electric driving force is proportional to the presynaptic membrane potential instead of the postsynaptic potential [8]. This means that for a saturated synapse,  $g_{syn} = g_0$  for  $n > n_0$  [5], the drive to neuron 2 is proportional to  $x_1$ . Neuron 2 has access to information about the input that normally would not cross the synapse, and that is also not present in the spike train of neuron 1. For the parameters used in Fig. 1, this did not significantly change the results. Second, the value of the synaptic conductance is essentially a step function of the neurotransmitter concentra-

tion  $n(t)$ :  $g_{syn} = 0$  for  $n < 4$  and  $g_{syn} = 0.1$  for  $n > 4$ . Again, this is not a critical feature, for a more gradual dependence on  $n$  (a lower  $\lambda$  value), similar results were obtained. Third, the threshold for neurotransmitter release is  $x_{thr} = -1$ , and is below the ‘‘afterhyperpolarization’’ of the model neuron during regular spiking. In cortical synapses the threshold was, say, between  $-50$  and  $0$  mV, corresponding to  $x_{thr}$  between 0 and 1. However, for these values, similar results could still be obtained when the value of  $n_0$  was chosen appropriately. The present value,  $x_{thr} = -1$ , may be appropriate for graded synapses, such as, for instance in the retina [9]. Therefore, the results of ERA are expected to hold for more general synaptic dynamics [10].

### III. CONCLUSION

In summary, the main premise of ERA remains true: the input signal may be hidden at one processing stage only to be recovered at a later stage. Their results also indicated that information may be encoded in spike trains at vastly different temporal resolutions. To decode this information, more sophisticated methods may be required, such as, for instance, those based on return maps. However, the data processing inequality still remains valid. Here we proposed a method by which ‘‘hidden’’ information can be extracted from spike trains, and showed in an example that the data processing inequality is satisfied. More study is needed to determine how useful this reconstruction method is, and what its possible neural correlates are.

### ACKNOWLEDGMENTS

I thank Terry Sejnowski and Jorge José for their advice, Arnaud Delorme for reading the manuscript, and Misha Rabinovich and Reynaldo Pinto for their comments on the manuscript and for providing Ref. [10] prior to publication. This work was supported by the Sloan-Swartz Center for Theoretical Neurobiology.

- 
- [1] M. N. Shadlen and W. T. Newsome, *J. Neurosci.* **18**, 3870 (1998).  
 [2] M. C. Eguia, M. I. Rabinovich, and H. D. I. Abarbanel, *Phys. Rev. E* **62**, 7111 (2000).  
 [3] A. Borst and F. Theunissen, *Nat. Neurosci.* **2**, 947 (1999).  
 [4] A. Destexhe, Z. F. Mainen, and T. J. Sejnowski, *Neural Comput.* **6**, 14 (1994).  
 [5] The model equations for neurons 1 and 2 are as given below Eq. (15) of ERA with  $J_{dc1} = J_{dc2} = 3.4$ . We use the same notation as in ERA. The input signal is a synaptic current,  $J_1(t) = J_0 \sum_i \Theta(t - t_i) [(t - t_i)/\tau] e^{-(t - t_i)/\tau}$ ; here  $t$  is the time,  $t_i$  is the  $i$ th input spike time,  $\Theta$  is the Heaviside function  $\Theta(x) = 1$  for  $x > 0$  and  $\Theta(x) = 0$  for  $x < 0$ ,  $\tau = 10$ , and  $J_0 = -0.05$ . The spike time  $t_i$  was generated by a  $\gamma$  process of order 2 with an average interspike interval equal to 1000. The synaptic current in neuron 2 induced by neuron 1 is  $J_2(t) = g_{syn}(x_{rev} - x_1(t))$ ; here  $g_{syn} = g_0 / \{1 + \exp[-\lambda(n(t) - n_0)]\}$  is the synaptic conductance,  $x_1$  is the membrane potential of presynaptic neuron 1,  $n$  is the neurotransmitter concentration given by

$dn/dt = \Theta(x_1(t) - x_{thr})(x_1(t) - x_{thr}) - \alpha n(t)$ ,  $\alpha = 0.05$ ,  $g_0 = 0.1$ ,  $\lambda = 50$ ,  $n_0 = 4$ , and  $x_{rev} = 3$ . The set of equations was integrated using a fourth order Runge-Kutta method [*Numerical Recipes* (Ref. [6]), with time step  $dt = 0.01$ ].

- [6] W. H. Press, S. A. Teukolsky, W. T. Vetterling, and B. P. Flannery, *Numerical Recipes* (Cambridge University Press, Cambridge, 1992).  
 [7] T. M. Cover and J. A. Thomas, *Elements of Information Theory* (Wiley, New York, 1991).  
 [8] The formula for the synaptic current into neuron 2,  $J_2 = g_{syn}(x_{rev} - x_1)$ , in Ref. [2] contained a typographical error. However, the numerical simulations in Ref. [2] were performed with the correct equation,  $J_2 = g_{syn}(x_{rev} - x_2)$  [M. I. Rabinovich, (private communication)].  
 [9] G. M. Shepherd, *The Synaptic Organization of the Brain* (Oxford University Press, New York, 1998).  
 [10] M. I. Rabinovich, R. D. Pinto, E. Tumer, G. Stiesberg, R. Huerta, H. D. I. Abarbanel, and A. I. Selverston (unpublished).